Biocatalysis and Agricultural Biotechnology 75 (2026) 104141

Contents lists available at ScienceDirect

Biocatalysis and Agricultural Biotechnology

journal homepage: www.elsevier.com/locate/bab

Dynamic modelling of L-threonine production by *E. coli* using whey and fish hydrolysates as substrates

Jhon Fredy Vélez Blandón [a], Silvia Ochoa [b], Claudia Patricia Sánchez Henao [a], José Edgar Zapata Montoya [a,*]

[a] Nutrition and Food Technology Research Group, Pharmaceutical and Food Sciences Faculty, Universidad de Antioquia, Medellín, 50010, Colombia
[b] SIDCOP Research Group, Engineering Faculty, Universidad de Antioquia, Medellín, 050010, Colombia

ARTICLE INFO

Keywords:
Essential amino acids
Kinetic modelling
Optimization
Bioprocess
Agro-industrial wastes

ABSTRACT

L-Threonine is an essential amino acid widely used in food, animal feed, cosmetics and medicine, which is mainly produced by microbial fermentation. In this work, the potential of L-threonine production from a culture media previously designed that uses agricultural and fishery wastes is studied at bioreactor scale (7.5L). Batch and fed-batch experiments were carried out using whey as carbon source and Red Tilapia (*Oreochromis sp.*) viscera hydrolysates, as nitrogen source. The experimental data obtained were used for developing a low-structure kinetic model which comprises the mass balances for the metabolites and 34 parameters that were identified. A two-step procedure for parameter identification was implemented. First, a general set of parameters (independently of the operating mode) was found. Second, the 10-most sensitive parameters were identified, specifically for each operating mode. The model proposed in this work allowed to properly describe the kinetics of biomass production, sugar consumption and L-threonine production, and it will be used in a future for the optimization and control of the bioprocess.

1. Introduction

Dairy and Fish industry are very important sectors of the Colombian economy. Whey is the principal waste from the dairy industry, where approximately 10 L of whey are obtained per kg of cheese produced (Zoppellari and Bardi, 2013). Degradation of whey causes both, a high chemical and biological oxygen demand, ranging from 60 to 80 g/L and 40 to 50 g/L, respectively (Zafar et al., 2005). Although whey might be used as animal feed and/or fertilizer, due to the high volumes produced, it has been recognized as an important environmental problem worldwide. In the Colombian context, cheese production has increased from 10,450 to 12,800 million kg between 2017 and 2020, which represents a very important increase in whey production (González et al., 2020). Therefore, it is necessary to keep finding approaches to use whey, for transforming it into valuable products while minimizing its environmental impact. On the other hand, byproducts of the fish industry represent between 50 and 70% of the weight of the animal, of which generally, only 30% is used, while the remaining 70% is discarded as waste (Villamil et al., 2017). This situation makes it necessary to search for profitable and environmentally friendly methods that allow the use of this type of waste. Production of hydrolysates is one of the alternatives for the use of these by-products, given that these peptides have great potential as value-added ingredients for the pharmaceutical and food industry, as they are considered safe, nutritionally healthy, low cost and with therapeutic benefits (Arias

* Corresponding author.
E-mail address: jhonf.velez@udea.edu.co (J.E. Zapata Montoya).

https://doi.org/10.1016/j.bcab.2026.104141
Received 21 July 2025; Received in revised form 5 April 2026; Accepted 24 June 2026
Available online 25 June 2026

et al., 2023; Opheim et al., 2015). The aquaculture production in Colombia has increased from 82,622 to 179,351 ton in the period 2011-2020, which means also an increasing on the amount of wastes produced (Minagricultura, 2021). Roughly speaking, around 57% w/w from the total catch (after filleting it), are wastes. From those, approximately 12-18% are viscera (Zapata Montoya and Franco Sanchez, 2022).

In a previous work by the present authors, L-threonine (THR) production from whey and Red Tilapia (*Oreochromis sp.*) Viscera Hydrolysates (RTVH) was investigated, at lab scale (Vélez Blandón et al., 2023). There, through an experimental design and subsequent analysis, it was shown the technical feasibility of using whey and RTVH to produce L-threonine by *E. coli* ATCC® 21277™. Furthermore, it was pointed out the need of applying modelling tools in order to increase the process understanding as a path to improve the process yield. Recent research on L-threonine production has demonstrated significant advances in both strain engineering and alternative substrate utilization. Zhao et al. (2025) comprehensively reviewed engineering strategies for *E. coli* and *C. glutamicum*, reporting record titters up to 170.3 g/L through systematic metabolic optimization. The economic viability of using low-cost substrates has gained particular attention, as substrate costs typically represent 20-40% of total fermentation expenses. Recent studies have shown promising results with agro-industrial wastes: Jin et al. (2025) achieved 92.46 g/L from untreated cane molasses, Liu et al. (2024) produced 67.63 g/L using engineered *C. glutamicum*, and Song et al. (2024) reached 118.2 g/L through quorum sensing systems. These advances underscore the current trend toward sustainable amino acid production from waste-derived substrates.

It is well known that modelling and simulation are very helpful tools for understanding and predicting the behaviour of biological systems. In this direction, our research group is currently working in two fronts: the use of metabolic modelling and the development of a dynamic based first principles model. The first approach is expected to allow the understanding of the effect that complex substrates, as well as key variables (i.e. such as precursors, promoters, dissolved oxygen and others) have on the threonine biosynthesis pathway, in order to propose strategies to increase its yield. Meanwhile, the goal of the latter (which is the one addressed in the current work), is to build a dynamic model of the process suitable to be used in a future work for optimizing the process operation at the macroscopic scale (i.e. determining optimal feeding profiles that maximizes the productivity). First principles-based dynamic models are important tools useful to understand, predict, and optimize the behaviour of the main process variables in chemical as well as in biochemical processes, while reducing the need of excessive experimentation saving both, time and resources. Such models play a critical role in the optimization and control of fermentation processes in order to assure a proper environment to the cells for promoting the desired metabolite production and increasing product quality, while minimizing the formation of undesired by-products. According to Almquist et al. (2014), several biological processes of importance (such as the metabolism of a cell culture during a batch and/or fed-batch process, cellular stress responses, or the decision making during the cell cycle), are non-stationary in their nature.

Some relevant previously reported works in the development/use of kinetic models for essential amino acids production are described. In the work by Özilgen (1988), experimental data previously reported were used for predicting the dynamic behaviour of nine different amino acids, obtained from microorganisms modified to be overproducers. Recent developments in bioprocess modelling have demonstrated the value of mechanistic and hybrid approaches for fermentation optimization (Du et al., 2022; Mahanty, 2023), though these typically demand greater computational resources than low-structured models. The Luedeking Piret model was found to be valid to represent the amino acids production data, which indicated that metabolites production was non-growth associated (Luedeking and Piret, 2000). Substrate was consumed mainly for growth and amino acids production, although amino acids are also consumed as a substrate in the first hours of fermentation. In the work by Liu et al. (2013), a dynamic unstructured model of the process was used for calculating the optimal feeding profiles for L-isoleucine in order to maximize the accumulation of L-threonine in the growth phase. On the other hand, Carranza-Saavedra et al. (2021) studied different carbon sources (including lactose and whey) to produce L-valine using genetically modified *E. coli* (ATCC® 13005™).

A variety of models have been reported in other cases of microbial amino acid production using agro-industrial waste, for example, the case of the study on obtaining xylitol with a strain of *Kluyveromyces marxianus* and palm oil hydrolysate as substrate (Manaf et al., 2023), or the case of the study on cocoa bean fermentation mechanisms by kinetic modelling for the standardisation of this process in the food industry (Moreno-Zambrano et al., 2022), among other reported cases. However, a review of the subject in open-access scientific literature shows that low-level models have not been specifically used to study the production of L-threonine with *E. coli* using complex substrates such as whey and fish hydrolysates.

In this work, mass balances for each biochemical species are written, which are complemented by using kinetic expressions for the rates at which the biochemical reactions take place. A low structured kinetic model (according to the classification by Novak (2015)) was preferred. As our purpose in a future work is to use the developed model for a real-time optimization application, we seek to have a good balance between the predictive capability and the computationally efficiency of the model. Growth and substrate consumption kinetics were modelled using Contois kinetic model, whereas Luedeking-Piret equation was used for modelling product formation.

2. Materials and methods

2.1. Microorganism

Escherichia coli ßIM-4 (*E. coliB*) strain was used, which was obtained from the ATCC® 21277™ reservoir. Then, it was modified by UV radiation to increase the production of L-threonine and its resistant to high concentrations of the α-amino-ß-hydroxyvaleric acid (i.e. higher than 1 mg/L) (Shio et al., 1971).

2.2. Culture media and growth conditions

Activation of *E. coliB* was carried out at 37°C and 100 rpm in 4 passes (varying the volume): pass 1 (10 mL, nutrient broth), pass 2 (50 mL, nutrient broth), pass 3 (50 mL, working complex medium), pass 4 (200 mL, working complex medium). Prior to each passage, the biomass produced was extracted by centrifugation at 9000 rpm and 4°C during 5min, and then it was re-suspended in the corresponding culture medium. During the last pass, THR production was checked as an indicator of metabolism activation to be able to use it as inoculum in the bioreactor. After *E. coli B* activation, it was inoculated into the Complex Production Medium (CPM) containing whey and RTVH, prepared according to the methodology described in a previous work (Vélez Blandón et al., 2023). For this, 3.5L of CPM were placed in a 7.5 L bioreactor (BioFlo® & Celligen™ 310, Eppendorf, Germany). The composition was: 7.3 g/L of glucose, 8.2 g/L of whey, 200 ml/L of RTVH, 3.9 g/L of $(NH_4)_2SO_4$, 2 g/L of KH_2PO_4, 1 g/L of $MgSO_4$, 0.004 g/L of $FeSO_4$, 0.0022 g/L of $MnSO_4$, 0.3 g/L of L-proline (PRO), 0.001 g/L of thiamine, 0.1 g/L of L-isoleucine (ILE) and 0.1 g/L of L-methionine (MET) (Vélez Blandón et al., 2023).

2.3. Batch and fed-batch operation

Batch and fed-batch experiments were carried out by duplicate in order to gather experimental data for identifying the model parameters. In all experiments, dissolved oxygen was controlled around 20% by varying the agitation and aeration from 300 to 420 rpm (Lee et al., 2006; Wanga et al., 2014). pH was controlled at a value of 7 by addition of NaOH (1M) or H_2SO_4 (1M), as required (Noor et al., 2013) in CPM. Meanwhile, the temperature was maintained at 36°C. Batch experiments were conducted for 24 h. Samples were taken every hour during the first 6 h of the process, then every 2 h until 12 h and then every 4 h until the end of the process (24 h).

For the fed-batch experiments, a feeding medium was prepared as follows: 19.82 g/L of glucose, 22.18 g/L of whey, 14.39 g/L of $(NH_4)_2SO_4$, 5.44 g/L of KH_2PO_4, 2.72 g/L of $MgSO_4$, 0.01 g/L of $FeSO_4$, 0.006 g/L of $MnSO_4$, 0.11 g/L of PRO, 0.001 g/L of thiamine, 0.08 g/L of ILE, and 0.08 g/L of MET. A batch stage (as previously described) was carried out for 8 h. Then the feed was started, keeping a constant feed flow rate of 0.0468 L/h during 22 h. Samples were periodically taken (in a similar manner as for the batch experiments), until the final process time was reached (30 h). All samples taken were centrifuged at 9000 rpm and 4°C during 5 min (Zhu and Shimizu, 2005) and the supernatant was stored for subsequent analysis for sugars and amino acids quantification.

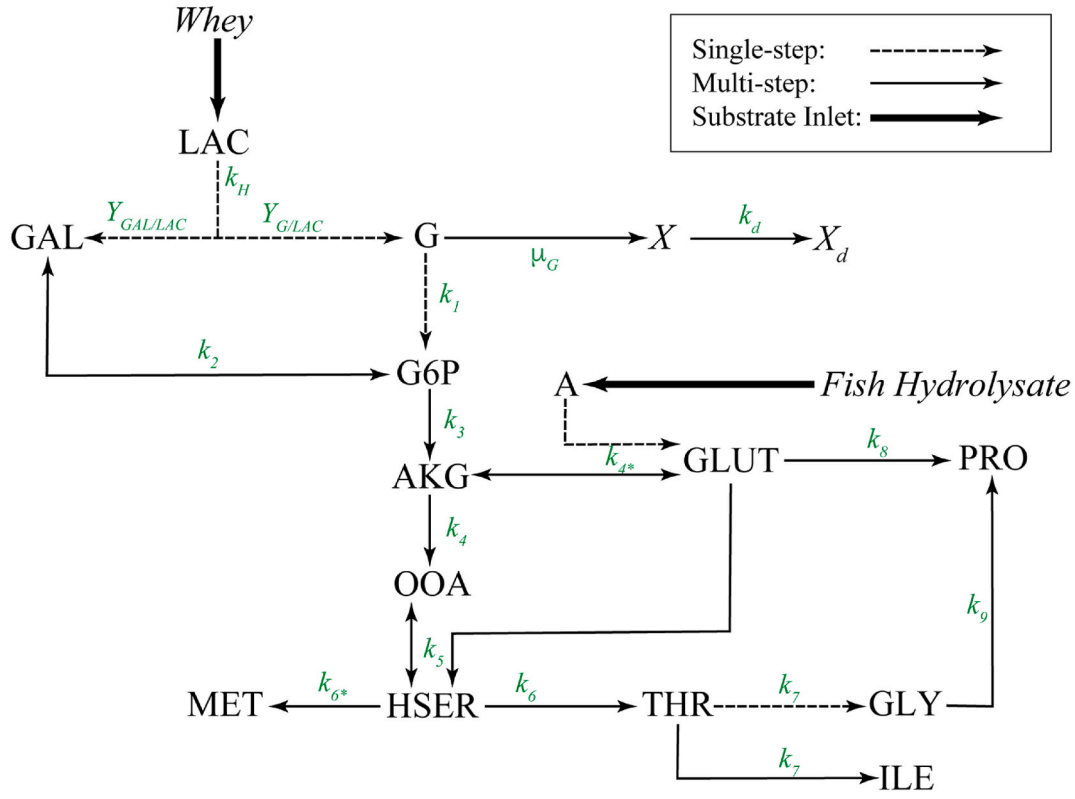

Fig. 1. Simplified pathway for Threonine production from whey and Red Tilapia Viscera Hydrolysates (fish hydrolysates). LAC (D-lactose), GAL (D-galactose), G (D-glucose), X (biomass), G6P (glucose 6-phosphate, AKG (alpha-ketoglutarate), OOA (Oxaloacetate), HSER (L-homoserine), MET (L-methionine). THR (L-threonine), ILE (L-isoleucine), GLY (glycine), PRO (L-proline), GLUT (L-glutamate), A (nitrogen source).

2.4. Analytical techniques

Biomass was determined by measuring the optical density at 600 nm (OD_{600}) using a Genesys 10S UV-VIS spectrophotometer (Thermo Scientific - United States). The OD_{600} data were converted using the factor $0.775 g_{DCW}/L{\cdot}UA$, obtained with the dry weight method applied to the strain used (Manzoor et al., 2017). For subsequent analysis, the samples were centrifuged at 9,000 rpm for 10 min and filtered using a 0.2 μm cellulose acetate filter. The sugars' content and amino acids were quantified in the supernatant. Glucose (G), galactose (GAL) and lactose (LAC) were determined by HPLC (Agilent 1200, Agilent Technologies) using an Aminex HPX-87H (7.8 × 300 mm, Bio-Rad) column and a refraction index detector (RID- G1362A). The mobile phase used was 5 mM H_2SO_4 at 0.6 mL/min and 35°C (Li et al., 2019). Amino acids were determined as described in a previous work (Vélez Blandón et al., 2023).

2.5. Dynamic model

In this section, the developed low-structured kinetic model is presented. The model is composed mainly of mass balances for the extracellular species and for the intracellular metabolites considered in the simplified pathway shown in Fig. 1.

The following assumptions were made for the development of the mathematical model:

- Lactose (LAC) is the initial substrate which is then broken down into Glucose (G) and Galactose (GAL) by enzymatic action (i.e. β-galactosidase), according to the following reaction:

$$LAC \xrightarrow{k_H} Y_{G/LAC}G + Y_{GAL/LAC}GAL$$

$Y_{G/LAC}$ and $Y_{GAL/LAC}$ are the stoichiometric yields of Glucose and Galactose from Lactose, respectively. Additionally, the hydrolysis kinetic rate coefficient is expressed as $k_H = \frac{k_h}{K_{mh}+LAC}$, where k_h and K_{mh} are a kinetic and a Michaelis–Menten constant for hydrolysis, respectively.

- The intracellular metabolites considered in the model are only those participating/involved in THR production, according to the reduced pathway shown in Fig. 1.
- Homogeneous composition in the fermenter (perfect mixture).
- The dynamics of both the absorption of nutrients by the microorganisms and the diffusion of metabolites from the microorganisms into the culture medium are neglected.
- Stoichiometric yields are assumed in the reactions.
- The kinetics described represent the average behaviour of the cells in culture.
- Density of the culture medium in the fermenter remains constant.
- Other metabolic reactions not included in the pathway are modelled through degradation kinetics.

In the following, the total mass balance and component mass balances are formulated as the core of the dynamic model proposed. Constitutive equations (i.e. kinetic expressions) complement the model. Model equations shown are written for the fed-batch case, in which a feed media is fed at a given-constant flowrate (F_{in}). The batch case arises from the same model equations by making $F_{in} = 0$.

Assuming constant density, the total mass balance results in:

$$\frac{dV}{dt} = F_{in} \tag{1}$$

where V is the volume and F_{in} is the volumetric flowrate.

A Mass Balance for the lactose (LAC) is given by:

$$\frac{dLAC}{dt} = \frac{F_{in} \cdot (LAC_{in} - LAC)}{V} - R_H \tag{2}$$

where LAC_{in} is the Lactose concentration in the feed and the hydrolysis rate R_H is expressed as suggested by Ladero et al. (2000):

$$R_H = \frac{k_h \cdot E \cdot LAC}{K_{mh} + LAC} \tag{3}$$

The dynamic behaviour for the Enzymes concentration (E) is given by:

$$\frac{dE}{dt} = R_E - \gamma E \tag{4}$$

where γ is a deactivation constant for the enzyme and the enzyme synthesis rate (R_E) is a function of biomass and lactose concentrations (Nath et al., 2016).

$$R_E = \frac{\alpha_E \cdot \mu_{max} \cdot LAC \cdot X}{K_{slac} + LAC} \tag{5}$$

where X is the biomass concentration, K_{slac} is a Monod constant for enzyme synthesis, α_E is a growth associated enzyme synthesis constant and μ_{max} is the maximum specific growth rate.

The mass balances for Glucose (G) and Galactose (GAL) result in:

$$\frac{dG}{dt} = \frac{F_{in} \cdot (G_{in} - G)}{V} + R_H \cdot Y_{\frac{G}{LAC}} - \frac{\mu \cdot X}{Y_{\frac{X}{G}}} - k_1 \cdot G \tag{6}$$

$$\frac{dGAL}{dt} = R_H \cdot Y_{\frac{GAL}{LAC}} - k_2 \cdot GAL - \frac{F_{in} \cdot GAL}{V} \tag{7}$$

where G_{in} is the glucose concentration in the feed, $Y_{\frac{X}{G}}$ is the biomass yield from glucose, $Y_{\frac{G}{LAC}}$ and $Y_{\frac{GAL}{LAC}}$ are the glucose and galactose yields from lactose, and k_1 and k_2 are kinetic constants. The specific biomass growth rate is expressed as:

$$\mu = \frac{\mu_{max} \cdot G}{K_s + G} \tag{8}$$

where Ks is a Monod constant for growth.

A mass balance for the biomass is given by:

$$\frac{dX}{dt} = \mu \cdot X - k_d \cdot X - \frac{F_{in} \cdot \mathrm{X}}{V} \tag{9}$$

where k_d is a cellular death constant.

The following equations represent the mass balances for the intracellular metabolites considered in the simplified pathway (see Fig. 1).

- *Mass balance for Glucose-6-phosphate (G6P)*

$$\frac{dG6P}{dt} = k_1 \cdot Y_{\frac{G6P}{G}} \cdot X \cdot G + k_2 \cdot Y_{\frac{G6P}{GAL}} 3X^*GAL - k_3 \cdot X \cdot G6P - \frac{F_{in} \cdot G6P}{V} \tag{10}$$

Where k_2 and k_3 is a kinetic constant and $Y_{\frac{G6P}{G}}, Y_{\frac{G6P}{GAL}}$ are the respective yields of G6P from G and GAL, respectively.

- *Mass balance for Alpha-Ketoglutarate (AKG)*

$$\frac{dAKG}{dt} = k_3 \cdot Y_{\frac{AKG}{G6P}} \cdot X \cdot G6P - k_4 \cdot X \cdot AKG - k_{4^*} \cdot X \cdot AKG \cdot A - \frac{F_{in} \cdot AKG}{V} \tag{11}$$

where k_4 and k_{4^*} are kinetic constants, A is the nitrogen-source concentration *(i.e.* ammonia), and $Y_{\frac{AKG}{G6P}}$ is the AKG yield from G6P.

- *Mass balance for Oxaloacetate (OOA)*

$$\frac{dOOA}{dt} = k_4 \cdot Y_{\frac{OOA}{AKG}} \cdot X \cdot AKG - k_5 \cdot X \cdot OOA \cdot GLUT - \frac{F_{in} \cdot OOA}{V} \tag{12}$$

where k_5 is a kinetic constant, $Y_{\frac{OOA}{AKG}}$ is the OOA yield from AKG and GLUT is the Glutamate concentration.

- *Mass balance for Glutamate (GLUT)*

$$\frac{dGLUT}{dt} = k_{4^*} \cdot Y_{\frac{GLUT}{AKG}} \cdot X \cdot AKG \cdot A - k_5 \cdot X \cdot OOA \cdot GLUT \cdot \frac{M_{w,GLUT}}{M_{w,OOA}} - k_8 \cdot X \cdot GLUT - k_{D,GLUT} \cdot (GLUT - GLUT_{min}) - \frac{F_{in} \cdot GLUT}{V} \tag{13}$$

where k_8 is a kinetic constant, $Y_{\frac{GLUT}{AKG}}$ is the GLUT yield from AKG, $k_{D,GLUT}$ is a decomposition constant and $GLUT_{min}$ is the GLUT decomposition concentration threshold.

- *Mass balance for Homoserine (HSER)*

$$\frac{dHSER}{dt} = k_5 \cdot Y_{\frac{HSER}{OOA}} \cdot X \cdot OOA \cdot GLUT - (k_6 + k_{6^*}) \cdot X \cdot HSER - k_{D,HSER} \cdot (HSER - HSER_{min}) - \frac{F_{in} \cdot HSER}{V} \tag{14}$$

where k_6 and k_{6^*} are kinetic constants and $Y_{\frac{HSER}{OOA}}$ is the HSER yield from OOA. $k_{D,HSER}$ is a decomposition constant and $HSER_{min}$ is the HSER decomposition concentration threshold.

- *Mass balance for Threonine (THR)*

$$\frac{dTHR}{dt} = k_6 \cdot Y_{\frac{THR}{HSER}} \cdot X \cdot HSER - k_7 \cdot X \cdot THR - k_{D,THR} \cdot (THR - THR_{min}) - \frac{F_{in} \cdot THR}{V} \tag{15}$$

where $Y_{\frac{THR}{HSER}}$ is the yield of THR from HSER and k_7 is a kinetic constant. $k_{D,THR}$ and THR_{min} are a decomposition constant and a decomposition concentration threshold for THR.

- *Mass balance for Glycine (GLY)*

$$\frac{dGLY}{dt} = k_7 \cdot X \cdot Y_{\frac{GLY}{THR}} \cdot THR - k_9 \cdot X \cdot GLY - k_{D,GLY}(GLY - GLY_{min}) - \frac{F_{in} \cdot GLY}{V} \tag{16}$$

where $k_{D,GLY}$ is a decomposition constant for Glycine, k_7 is a kinetic constant, $Y_{\frac{GLY}{THR}}$ is the GLY yield from THR and GLY_{min} is GLY decomposition concentration threshold.

- *Mass balance for Proline (PRO)*

$$\frac{dPRO}{dt} = \frac{F_{in} \cdot (PRO_{in} - PRO)}{V} + k_8 \cdot Y_{\frac{PRO}{GLUT}} \cdot X \cdot GLUT + k_9 \cdot X \cdot GLY \cdot Y_{\frac{PRO}{GLY}} - k_{D,PRO} \cdot (PRO - PRO_{min}) \tag{17}$$

where PRO_{in} is the proline concentration in the feed, $k_{D,PRO}$ is a decomposition constant for Proline, PRO_{min} is the PRO decomposition concentration threshold and $Y_{\frac{PRO}{GLUT}}$ and $Y_{\frac{PRO}{GLY}}$ are the PRO yields from GLUT and GLY, respectively.

- *Mass balance for Methionine (MET)*

$$\frac{dMET}{dt} = \frac{F_{in} \cdot (MET_{in} - MET)}{V} + k_{6^*} \cdot Y_{\frac{MET}{HSER}} \cdot X \cdot HSER - k_{D,MET} \cdot (MET - MET_{min}) \tag{18}$$

where MET_{in} is the Methionine concentration in the feed, $k_{D,MET}$ is a kinetic decomposition constant, MET_{min} is the MET decomposition concentration threshold, and $Y_{\frac{MET}{HSER}}$ is the MET yield from HSER.

- *Mass balance for Isoleucine (ILE)*

$$\frac{dILE}{dt} = \frac{F_{in} \cdot (ILE_{in} - ILE)}{V} + k_7 \cdot Y_{\frac{ILE}{THR}} \cdot X \cdot THR - k_{D,ILE} \cdot (ILE - ILE_{min}) \tag{19}$$

where ILE_{in} is the Isoleucine concentration in the feed, $k_{D,ILE}$ is a decomposition constant, $Y_{\frac{ILE}{THR}}$ is the ILE yield from THR and ILE_{min} is the ILE decomposition concentration threshold.

- *Mass balance for the nitrogen source (A)*

$$\frac{dA}{dt} = \frac{F_{in} \cdot (A_{in} - A)}{V} - \frac{k_{4^*} \cdot M_{w,A} \cdot X \cdot AKG \cdot A}{M_{w,AKG}} \tag{20}$$

where A_{in} is the ammonia concentration in the feed, $M_{w,A}$ and $M_{w,AKG}$ are the ammonia and alpha-ketoglutarate molecular weights, respectively.

2.6. Parameter identification

After setting the model structure (see equations (1)–(20)) parameter identification was performed in order to find the most suitable value for the 34 parameters that are part of the model, independently of the operation mode (i.e. batch vs fed-batch). It is well known that the operation mode impacts the behaviour of the microorganisms, and therefore, different yields can be obtained. In this work, the purpose is to develop a general model that can be used independently of the operating mode, by making minor modifications. Although the model structure is general for the process, the value of the parameters is usually adjusted depending on the operation mode. In order to propose a suitable predictive model that requires minor modifications when the operating mode changes, a sensitivity analysis was performed in order to find only those model parameters that are highly sensitive to the operating mode and therefore require to be specifically determined when changing the operating mode (i.e. from batch to fed-batch). The identification procedure proposed in Ochoa et al. (2007) was applied in order to determining the optimal values for the parameters. First, a "general optimization" routine was solved, which included the use of experimental data from the batch as well as the fed-batch operation modes. Then, the sensitivity analysis allowed identifying those parameters highly dependable on the operation mode. Finally, a re-optimization procedure for finding the specific optimal values for those sensitive parameters was performed. As mentioned, a total of 34 parameters must be

identified. The optimization routine for finding the general parameter set and the re-optimization for identifying the sensitive parameters were performed using the Molecular Inspired Parallel Tempering (MIPT) Algorithm (Ochoa et al., 2010). The objective function (F_{obj}) minimized (see equation (21)) was defined considering the normalized Mean of the Squared Error (MSE) for the m measured variables (see equation (22)) (e.g. biomass, glucose, lactose, galactose, threonine, proline, methionine, isoleucine, and glycine), as follows:

$$F_{obj} = \sum_{j=1}^{m} MSE_j \tag{21}$$

The normalized MSE for each measured variable *(j = 1, 2, …, 9)* is calculated as:

$$MSE_j = \frac{1}{n} \cdot \sum_{i=1}^{n} \left[\frac{y_{exp,i} - \widehat{y}_i}{\max\left(y_{exp,i}\right)} \right]^2 \tag{22}$$

where $y_{exp,i}$ and $\widehat{y}_i$ (for i = 1, 2, …, n) are the experimental data used for parameter identification and the value predicted by the model for the variable *y*. *n* is the number of available experimental data sets used. For carrying out the parameter identification, the duplicate batch and the duplicate fed-batch experiments described in section Batch and Fed-batch operation, were used.

3. Results

Figs. 3 and 5 show the consumption of D-glucose and D-lactose for batch and fed-batch operations respectively; the behaviour observed suggests that the two substrates are not consumed simultaneously; rather, they follow a consumption hierarchy in which D-glucose is depleted first, as it is the carbon source used by *E. coli* during the exponential growth phase. The consumption of D-lactose is only switched on when glucose is depleted and the *lac* operon is activated (Ammar et al., 2018; Deutscher, 2008; Doshi et al., 1997; Kremling et al., 2015), as it is the carbon source used during the L-threonine production phase. Furthermore, the depletion of D-glucose takes place together with the depletion of L-methionine (see Figs. 4f and 6f), L-isoleucine (see Figs. 4b and 6b) and L-proline (see Figs. 4d and 6d). These have an important role as inducers in the L-threonine production (Shiio et al., 1971). Whilst L-threonine production also started (see Figs. 4a and 6a). Additionally, the fish hydrolysate used was composed mainly of peptides and free amino acids (Arias et al., 2023; Gómez et al., 2019), which are incorporated into the metabolism of *E. coli* (Thompson and Maurizi, 1994; Yang et al., 2024; Zhao et al., 2025). This shows that *E. coli* uses D-lactose and fish hydrolysates as substrates, whilst L-methionine, L-isoleucine and L-proline have an important role in directing the synthesis and degradation pathways of L-threonine during the production of this amino acid.

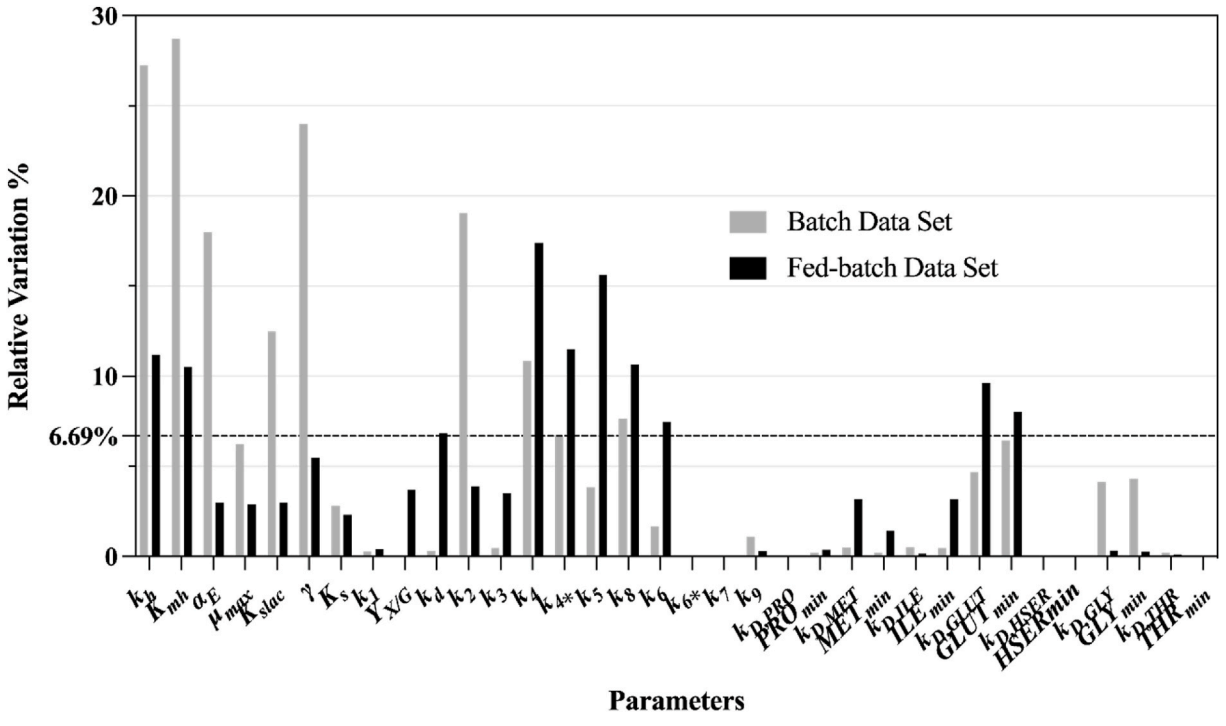

Fig. 2. Sensitivity analysis for batch and fed-batch operations of the parameters presented in the implemented model.

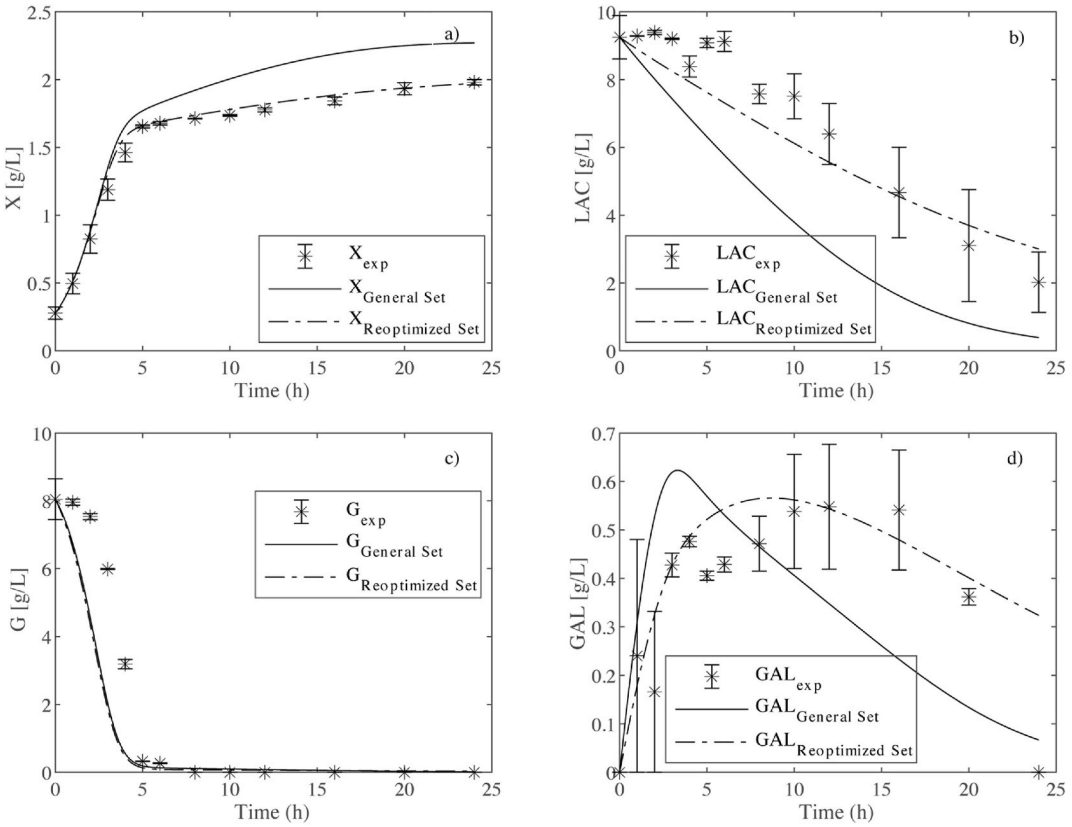

Fig. 3. Model predictions vs experimental data for **batch** fermentations for **a)** Biomass, **b)** Lactose, **c)** Glucose, **d)** Galactose. Error bars show the variation of two independent fermentations (considering the Median Absolute Deviation, MAD). General set of parameters (solid line) and re-optimized set (dash-dotted line).

Figs. 4 and 6, shows the production of L-threonine for batch and fed-batch processes. During the batch operation, approximately 177 mg/L of L-threonine was produced, whereas in the fed-batch operation, approximately 234 mg/L was obtained. This indicates a 32% increase in L-threonine production in the fed-batch operation compared to the batch operation. Meanwhile, in the batch operation, maximum L-threonine production was achieved 10 h after the start of fermentation, whereas in the fed-batch operation, maximum L-threonine production was achieved at 14 h, as the fed-batch operation started 8 h after the fermentation began; this indicates that the strategy employed for the fed-batch operation not only increased L-threonine production but also extended it.

Table 1 shows the parameter identification results. The first column shows the nomenclature/symbols used. Second column shows the "general parameter set" (i.e. found by running the parameter identification using both, the batch and fed-batch experimental data simultaneously). The bold variables indicate the most sensitive parameters detected during the sensitivity analysis, which therefore required a re-optimization step (performed by using each data set independently). Finally, the third and fourth columns show the re-optimized set of parameters for the batch and fed-batch cases.

A sensitivity analysis by perturbation method was performed in order to find the most sensitive parameters. Results of this analysis can be seen in Fig. 2, where the relative variation of the objective function is plotted against the list of parameters. From the relative variation for both data sets (i.e. batch and fed-batch data), the highest 25% of the values (corresponding to the third quartile of the data, i.e. 6.69% of relative variation) were considered as sensitive (Ochoa et al., 2025).

According to the sensitivity analysis, only 14 parameters from the general set of 34, were determined as sensitive parameters. Therefore, those 14- parameters were re-optimized for each identification data set independently (results shown in the last two columns of Table 1). During the independent re-optimization, it was found that four parameters from the sensitive parameters set (namely k_4, k_{4^*}, k_8 and $GLUT_{min}$) were already at an optimal value (i.e the corresponding to the general set). Therefore, at the end, for the case study analysed and to the light of the experimental data, it was concluded than only 10 parameters were sensitive.

Figs. 3 and 4 show the results for batch operation, meanwhile Figs. 5 and 6 show the results for fed-batch operation, respectively. In those, it is possible to compare the model fit when using the general-set of parameters (solid line) against the re-optimized set (dotted-dashed line) (i.e. where only the parameters found to be sensitive were re-optimized). In general terms, it is worth noting that the biomass behaviour is atypical, since the lag phase is not observed, thanks to the strategy of intensification in the inoculum concentration and metabolism activation (see Fig. 3a). Exponential growth phase was observed from 0 to 5 h, and the growth deceleration phase is prolonged from 5 to 24 h. During the exponential phase (0 to 5 h), it coincides with the accelerated and total consumption of

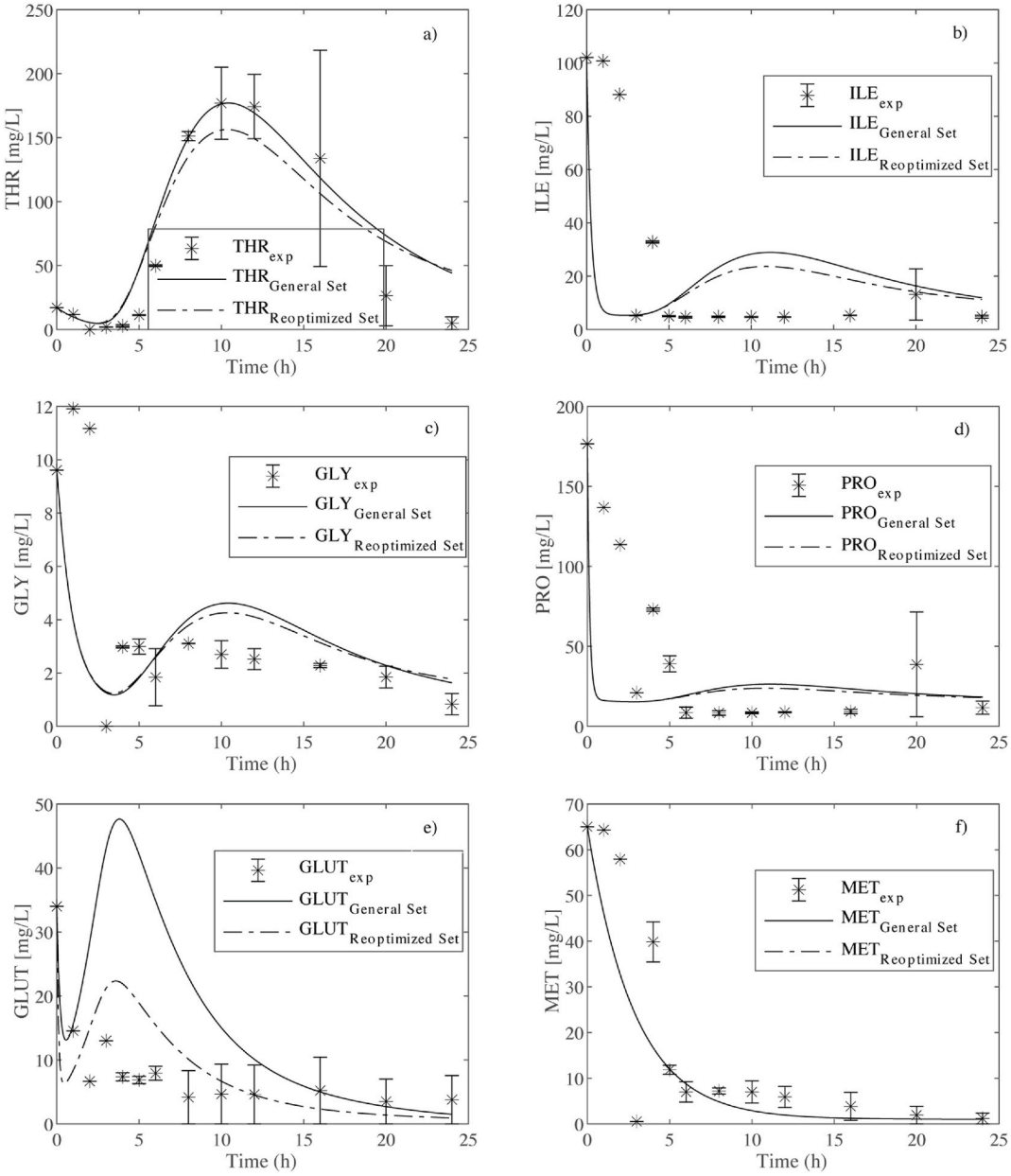

Fig. 4. Model predictions vs experimental data for **batch** fermentations for **a)** Threonine, **b)** Isoleucine, **c)** Glycine, **d)** Proline, **e)** Glutamate and **f)** Methionine. Error bars show the variation of two independent fermentations (considering the Median Absolute Deviation, MAD). General set of parameters (solid line) and re-optimized set (dash-dotted line).

glucose, and the deceleration growth phase with a slower consumption of lactose (5 to 24 h), showing that *E. coliB*, through a hierarchical metabolism (Poccia et al., 2014), consumes both glucose and lactose (whey) for its development and for the production of L-threonine, where the lactose consumption phase converges with the production phase of this amino acid. This behaviour was very similar regardless of the type of operating mode (batch vs. fed-batch). On the other hand, the L-threonine present at the starting of tests in the culture medium is completely consumed during the exponential growth phase (see Fig. 4a), as is the case with the inducers (L-isoleucine, L-proline and L-methionine) (see Fig. 4b–d and f respectively). Similarly, during the exponential growth phase, there was a marked consumption of free amino acids from fish hydrolysate, such as glycine and glutamate (see Figs. 4 and 6), showing that this substrate is indeed used as a substrate by *E. coliB*. The production of L-threonine started at the end of the exponential growth phase, making this amino acid a secondary metabolite not associated to cell growth for the *E. coliB* strain. On the other hand, during fed-batch operation, similar behaviours were observed for biomass and sugar consumption (see Fig. 5), L-threonine production and inducers consumption (see Fig. 6).

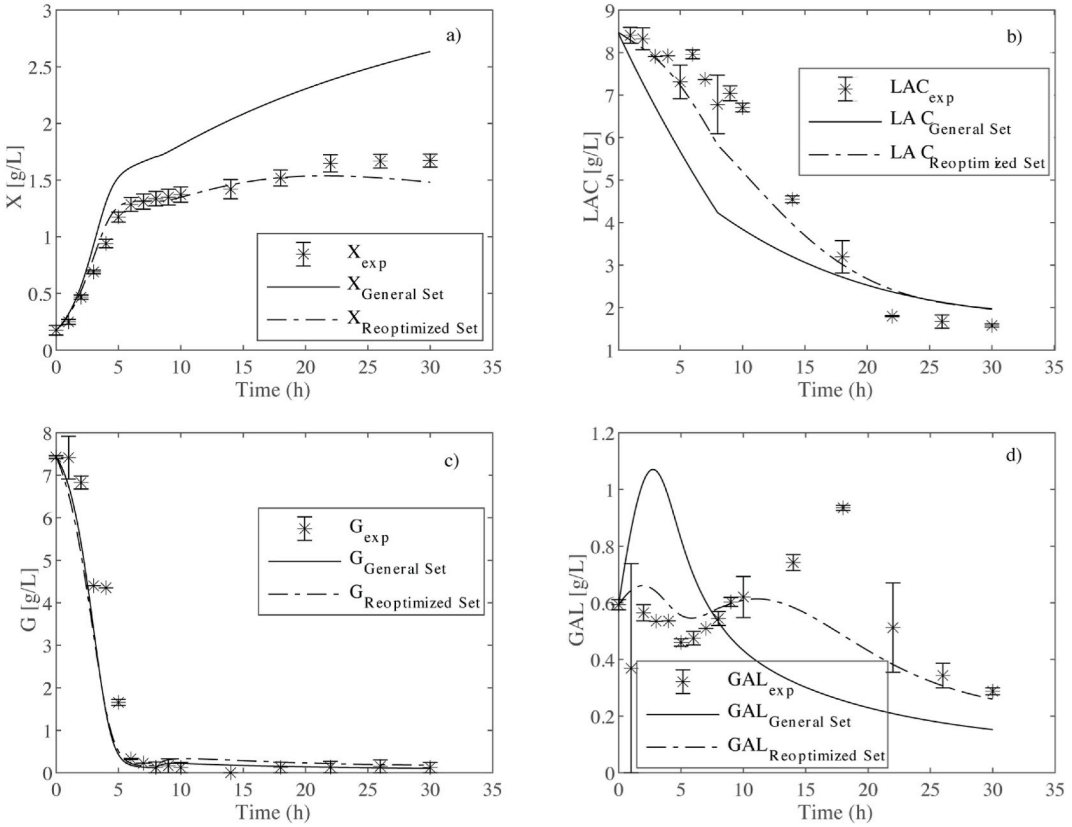

Fig. 5. Model predictions vs experimental data for **fed-batch** fermentations for **a)** Biomass, **b)** Lactose, **c)** Glucose, **d)** Galactose. Error bars show the variation of two independent fermentations (considering the Median Absolute Deviation, MAD). General set of parameters (solid line) and re-optimized set (dash-dotted line).

Continuing with the analysis, regarding the most-sensitive parameters, it is possible to observe that the kinetic constant for lactose hydrolysis (k_h) and the Michaelis–Menten constant for hydrolysis (K_{mh}) changed in opposite directions between batch and fed-batch operations. Specifically, kh increased in fed-batch operation while K_{mh} decreased, indicating that the lactose hydrolysis rate was higher for the fed-batch case than for the batch process. The K_{mh} (which is analogous to K_S in the Monod equation) exhibited opposite behaviour. This phenomenon can be attributed to the operational strategy of fed-batch mode, where maintaining low glucose concentrations avoids enzymatic inhibition by high sugar levels, favouring lactose breakdown while minimizing catabolite repression and acetate overflow metabolism (Eiteman and Altman, 2006).

The threonine biosynthetic pathway involves a complex network within the Aspartate family. From L-aspartate, the pathway branches to L-asparagine and Aspartate Semialdehyde, which serves as precursor for L-lysine and L-homoserine. L-methionine and threonine are both derived from L-homoserine, with threonine (the product of interest in the current investigation) serving as precursor for L-isoleucine and glycine, while also participating as a parallel activator for L-valine biosynthesis and other compounds necessary for biomass synthesis (Herrmann and Somerville, 1983; Liaw et al., 2007; Park and Lee, 2010). Fed-batch operation significantly enhances this enzymatic complex, causing the kinetic constants k_5, k_6, and $k_{D,GLUT}$ to increase considerably compared to batch mode. This enhancement can be explained by four interconnected mechanisms: (1) Fed-batch operation maintains lower glucose concentrations, which reduces catabolite repression and allows for more efficient amino acid biosynthesis through the aspartate pathway, while preventing the accumulation of inhibitory byproducts such as acetate that decrease pH and impair threonine production (Eiteman and Altman, 2006). (2) The higher k_5 and k_6 values observed in fed-batch mode reflect increased expression of threonine biosynthetic enzymes (aspartate kinase, homoserine dehydrogenase, threonine synthase) under nutrient-limited conditions. Modification of glycolysis to attenuate excessive flux has been shown to redirect carbon toward threonine biosynthesis (Xie et al., 2014), while betaine supplementation can further improve production by upregulating glucose-6-phosphate dehydrogenase (*zwf*), thereby enhancing cofactor availability for biosynthetic reactions (Li et al., 2019). (3) The variation in $k_{D,GLUT}$ reflects a metabolic adaptation where *E. coli* modulates its glucose uptake rates to optimize carbon flux through L-threonine biosynthetic pathways while avoiding acetate overflow metabolism. Recent modelling of dynamic substrate uptake demonstrates that cells adapt their consumption capacity in response to biomass density and substrate availability, maximizing biosynthetic efficiency under fed-batch conditions (Ibaceta et al., 2025). (4) These adaptive responses align with previously reported two-stage feeding strategies that control both the type and level of feeding nutrients to significantly improve fed-batch threonine production while minimizing byproduct formation (Liu

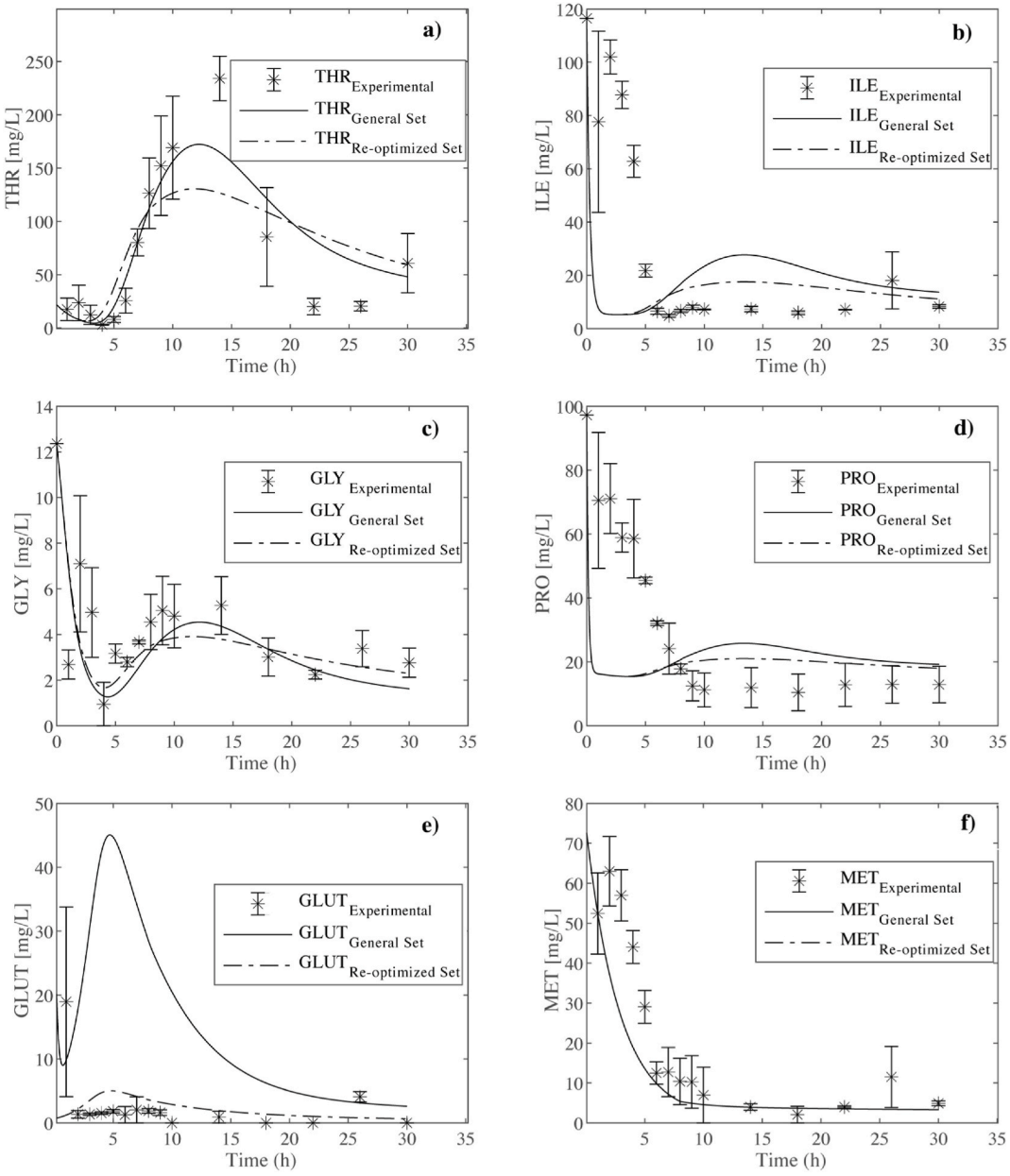

Fig. 6. Model predictions vs experimental data for **fed-batch** fermentations for **a)** Threonine, **b)** Isoleucine, **c)** Glycine, **d)** Proline, **e)** Glutamate and **f)** Methionine. Error bars show the variation of two independent fermentations (considering the Median Absolute Deviation, MAD). General set of parameters (solid line) and re-optimized set (dash-dotted line).

et al., 2013; Wanga et al., 2014). In contrast, batch operation exhibits inhibition effects by product accumulation, limiting the overall productivity of the bioprocess.

In general, the results obtained for batch and fed-batch operations show that the proposed model achieves an adequate fit for biomass production and consumption of glucose and lactose, and also reproduces the production and consumption of galactose. L-threonine production was also adequately described. Therefore, the proposed model adequately describes the studied bioprocess allowing its application to further studies associated with threonine optimization with *E. coli*. Figs. 5 and 6 show the results for the fed-batch case. Again, it is possible to compare the fit under the two scenarios (general set of parameters vs the re-optimized set).

It is important to highlight that while the proposed low-structured model provides valuable insights into the dynamic behaviour of the main process variables and enables targeted process optimization, it has some limitations. For example, as the substrates used are complex, their physicochemical characteristics can vary significantly, requiring re-optimization of sensitive parameters for each case. However, model equations are still valid due to their foundation in the first-principles (mass balances). Therefore, the model can be

Table 1
Parameter identification results for the model shown in equations (1)–(20).

Parameter (Units)	General Set	Batch (re-optimized)	Fed-batch (re-optimized)
$k_h\left(h^{-1}\right)$	0.014	**0.011**	**0.023**
$K_{mh}\left(gL^{-1}\right)$	2.501	**7.459**	**4.647**
α_E	8.178	**22.876**	**30.013**
$\mu_{max}\left(h^{-1}\right)$	0.950	0.950	0.950
$K_{slac}\left(gL^{-1}\right)$	32.046	**51.441**	**20.817**
$\gamma\left(h^{-1}\right)$	0.042	**0.069**	**0.139**
$K_s\left(gL^{-1}\right)$	4.063	4.063	4.063
$k_1\left(Lg^{-1}h^{-1}\right)$	0.190	0.190	0.190
$Y_{X/G}\left(gg^{-1}\right)$	0.215	0.215	0.215
$k_d\left(h^{-1}\right)$	0.003	**0.006**	**0.004**
$k_2\left(h^{-1}\right)$	0.327	**0.157**	**0.327**
k_3	0.210	0.210	0.210
k_4	0.079	0.079	0.079
k_{4^*}	0.039	0.039	0.039
k_5	1.871	**4.422**	**12.822**
k_8	0.000	0.000	0.000
k_6	0.244	**0.244**	**2.946**
k_{6^*}	0.000	0.000	0.000
k_7	0.235	0.235	0.235
k_9	6.697	6.697	6.697
$k_{D,PRO}$	7.212	7.212	7.212
PRO_{min}	0.013	0.013	0.013
$k_{D,MET}$	0.352	0.352	0.352
MET_{min}	0.001	0.001	0.001
$k_{D,ILE}$	3.877	3.877	3.877
ILE_{min}	0.005	0.005	0.005
$k_{D,GLUT}$	5.000	**9.667**	**41.575**
$GLUT_{min}$	0.000	0.000	0.000
$k_{D,HSER}$	0.000	0.000	0.000
$HSER_{min}$	0.010	0.010	0.010
$k_{D,GLY}$	0.100	0.100	0.100
GLY_{min}	0.100	0.100	0.100
$k_{D,THR}$	0.468	0.468	0.468
THR_{min}	0.000	0.000	0.000
MSE	0.7526 (batch) 0.8711 (fed-batch)	0.3926	0.3381

adapted to different substrate types and feeding strategies.

4. Conclusions

This work demonstrated the feasibility of using a low-structure kinetic model to study the production of L-threonine at the bioreactor scale with *E. coli* βIM-4 incorporating whey and Red Tilapia (*Oreochromis sp.*) viscera hydrolysate as substrates, independently of the operating mode (i.e. batch, fed-batch). This is the first study of its type in which a bioprocess involving the use of complex substrates for L-threonine production is modelled. At first, the proposed model was successful in adequately reproducing biomass production, sugar consumption and L-threonine production under batch and fed-batch operations. In a second step, the analysis of the kinetic parameters found allowed identifying that the type of operation affects some of these parameters, specifically related to the metabolism of the substrates and to the synthesis routes of some amino acids. This provides valuable information that requires the use of metabolic modelling for its verification. The results obtained here allow using this model in future studies associated with the optimization of L-threonine production with *E. coli* (i.e. optimization of feeding profile and soft-sensors development for monitoring) using whey and fish hydrolysate as substrates, at pilot plant scale.

CRediT authorship contribution statement

Jhon Fredy Vélez Blandón: Writing – review & editing, Project administration, Methodology, Investigation, Formal analysis, Data curation, Conceptualization. **Silvia Ochoa:** Writing – review & editing, Writing – original draft, Visualization, Supervision, Software, Methodology, Formal analysis, Data curation, Conceptualization. **Claudia Patricia Sánchez Henao:** Writing – review & editing, Project administration, Funding acquisition, Conceptualization. **José Edgar Zapata Montoya:** Writing – review & editing, Supervision, Conceptualization.

Declaration of competing interest

The authors declare that they have no known competing financial interests or personal relationships that could have appeared to influence the work reported in this paper.

Acknowledgments

We thankfully recognize the support provided by the Universidad de Antioquia through the calls “Thematic Research Projects 2020: Science and innovation in response to university and national challenges” (project No. 2020–33174), and the “Programmatic Call: Engineering and Technology 2019–2020” (project No. 2020–33781). The financial support from Insumos Ambientales S.A.S. and letters of interest on the subject from company Surcolat S.A. and Lateos la Fontana S.A.S.

Glossary

AKG	Alpha-ketoglutarate
CPM	Complex Production Medium
E. coliB	*Escherichia coli* ßIM-4
G	D-glucose
G6P	Glucose 6-phospate
GAL	D-galactose
GLUT	L-glutamate
GLY	Glycine
HSER	L-homoserine
ILE	L-isoleucine
LAC	D-lactose
MET	L-methionine
OOA	Oxaloacetate
PRO	L-proline
RTVH	Red Tilapia (*Oreochromis sp.*) Viscera Hydrolysates
THR	L-threonine
X	Biomass

Data availability

Data will be made available on request.

References

Almquist, J., Cvijovic, M., Hatzimanikatis, V., Nielsen, J., Jirstrand, M., 2014. Kinetic models in industrial biotechnology – improving cell factory performance. Metab. Eng. 24, 38–60. https://doi.org/10.1016/j.ymben.2014.03.007.

Ammar, E.M., Wang, X., Rao, C.v., 2018. Regulation of metabolism in *Escherichia coli* during growth on mixtures of the non-glucose sugars: arabinose, lactose, and xylose. Sci. Rep. 8 (1), 609. https://doi.org/10.1038/s41598-017-18704-0.

Arias, L., Sánchez-Henao, C.P., Zapata, J.E., 2023. Optimization of the separation conditions of antioxidant peptides from red tilapia (*Oreochromis spp.*) viscera on cross-flow filtration ceramic membranes. S. Afr. J. Chem. Eng. 45, 100–110. https://doi.org/10.1016/j.sajce.2023.05.002.

Carranza-Saavedra, D., Sánchez Henao, C.P., Zapata Montoya, J.E., 2021. Kinetic analysis and modeling of L-valine production in fermentation batch from *E. coli* using glucose, lactose and whey as carbon sources. Biotechnol. Rep. 31. https://doi.org/10.1016/j.btre.2021.e00642.

Deutscher, J., 2008. The mechanisms of carbon catabolite repression in bacteria. Curr. Opin. Microbiol. 11 (2), 87–93. https://doi.org/10.1016/j.mib.2008.02.007.

Doshi, P., Rengaswamy, R., Venkatesh, K.v., 1997. Modelling of microbial growth for sequential utilization in a multisubstrate environment. Process Biochem. 32 (8), 643–650. https://doi.org/10.1016/S0032-9592(97)00013-7.

Du, Y.-H., Wang, M.-Y., Yang, L.-H., Tong, L.-L., Guo, D.-S., Ji, X.-J., 2022. Optimization and Scale-Up of fermentation processes driven by models. Bioengineering 9, 473. https://doi.org/10.3390/bioengineering9090473.

Eiteman, M.A., Altman, E., 2006. Overcoming acetate in *Escherichia coli* recombinant protein fermentations. Trends Biotechnol. 24, 530–536. https://doi.org/10.1016/j.tibtech.2006.09.001.

Gómez, L.J., Gómez, N.A., Zapata, J.E., López-García, G., Cilla, A., Alegría, A., 2019. In-vitro antioxidant capacity and cytoprotective/cytotoxic effects upon Caco-2 cells of red tilapia (Oreochromis spp.) viscera hydrolysates. Food Res. Int. 120, 52–61. https://doi.org/10.1016/j.foodres.2019.02.029.

González, A., Peña, Y., Samacá, H., Leyva, F., Valderrama, P., 2020. Análisis Situacional Cadena Láctea.

Herrmann, K.M., Somerville, R.L., 1983. Amino Acids: Biosynthesis and Genetic Regulation. Addison-Wellesley Publishing Co., Inc., pp. 147–171

Ibaceta, M., Neudert, M.-R., Marques, N., Kahrer, S., Herwig, C., Steinboeck, A., 2025. The dynamic growth of bacterial cultures: real-time Bayesian estimation of substrate uptake rates in fed-batch fermentations of *E. coli*. Bioproc. Biosyst. Eng. https://doi.org/10.1007/s00449-025-03251-0.

Jin, X., Wang, S., Gao, Y., Qi, Q., Liang, Q., 2025. Combinatorial metabolic engineering of *Escherichia coli* to efficiently produce L-threonine from untreated cane molasses. Bioresour. Technol. 419, 132058. https://doi.org/10.1016/j.biortech.2025.132058.

Kremling, A., Geiselmann, J., Ropers, D., de Jong, H., 2015. Understanding carbon catabolite repression in *Escherichia coli* using quantitative models. Trends Microbiol. 23 (2), 99–109. https://doi.org/10.1016/j.tim.2014.11.002.

Ladero, M., Santos, A., García-Ochoa, F., 2000. Kinetic modeling of lactose hydrolysis with an immobilized β-galactosidase from *Kluyveromyces fragilis*. Enzym. Microb. Technol. 27, 583–592. https://doi.org/10.1016/S0141-0229(00)00244-1.

Lee, M.H., Lee, H.W., Park, J.H., Ahn, J.O., Jung, J.K., Hwang, Y. Il, 2006. Improved L-threonine production of *Escherichia coli* mutant by optimization of culture conditions. J. Biosci. Bioeng. 101, 127–130. https://doi.org/10.1263/jbb.101.127.

Li, Y., Zhang, D., Cai, N., Han, C., Mao, Q., Wang, T., Zhou, Q., Chen, N., Xie, X., 2019. Betaine supplementation improved L-threonine fermentation of *Escherichia coli* THRD by upregulating *zwf* (glucose-6-phosphate dehydrogenase) expression. Electron. J. Biotechnol. 39, 67–73. https://doi.org/10.1016/j.ejbt.2019.03.004.

Liaw, H.J., Bradshaw, J.S., Yang, Y., Mao, W., 2007. US7220571 *Escherichia coli* Which Over-produce L-threonine and Processes for the Production of L-threonine by Fermentation.

Liu, Jianhang, Liu, Jiao, Li, J., Zhao, X., Sun, G., Qiao, Q., Shi, T., Che, B., Chen, J., Zhuang, Q., Wang, Y., Sun, J., Zhu, D., Zheng, P., 2024. Reconstruction the feedback regulation of amino acid metabolism to develop a non-auxotrophic L-threonine producing *Corynebacterium glutamicum*. Bioresour. Bioprocess. 11, 43. https://doi.org/10.1186/s40643-024-00753-9.

Liu, S., Liang, Y., Liu, Q., Tao, T., Lai, S., Chen, N., Wen, T., 2013. Development of a two-stage feeding strategy based on the kind and level of feeding nutrients for improving fed-batch production of L-threonine by *Escherichia coli*. Appl. Microbiol. Biotechnol. 97, 573–583. https://doi.org/10.1007/s00253-012-4317-4.

Luedeking, R., Piret, E.L., 2000. A kinetic study of the lactic acid fermentation. Batch process at controlled pH. Biotechnol. Bioeng. 67, 636–644. https://doi.org/10.1002/(SICI)1097-0290(20000320)67:6<636::AID-BIT3>3.0.CO;2-U.

Mahanty, B., 2023. Hybrid modeling in bioprocess dynamics: structural variabilities, implementation strategies, and practical challenges. Biotechnol. Bioeng. 120, 2072–2091. https://doi.org/10.1002/bit.28503.

Manaf, S.F.A., Luthfi, A.A.I., Tan, J.P., Abdul, P.M., Jamali, N.S., 2023. Kinetic study and model of fermentation parameters affected growth and xylitol production in bioreactor by *Kluyveromyces marxianus* ATCC 36,907. Biomass Convers. Biorefinery 13, 7247–7263. https://doi.org/10.1007/s13399-022-02976-2.

Manzoor, A., Qazi, J.I., Haq, I.U., Mukhtar, H., Rasool, A., 2017. Significantly enhanced biomass production of a novel bio-therapeutic strain *Lactobacillus plantarum (AS-14)* by developing low cost media cultivation strategy. J. Biol. Eng. 11. https://doi.org/10.1186/s13036-017-0059-2.

Minagricultura, 2021. Acuicultura en Colombia, cadena de la acuicultura. Dirección De Cadenas Pecuarias, Pesqueras Y Acuícolas.

Moreno-Zambrano, M., Ullrich, M.S., Hütt, M.-T., 2022. Exploring cocoa bean fermentation mechanisms by kinetic modelling. R. Soc. Open Sci. 9. https://doi.org/10.1098/rsos.210274.

Nath, A., Chowdhury, R., Bhattacharjee, C., Maitra, M., 2016. Production of β-galactosidase in a batch bioreactor using whey through microbial route – characterization of isolate and reactor model. Periodica Polytech., Chem. Eng. 60, 298–312. https://doi.org/10.3311/PPch.8286.

Noor, R., Islam, Z., Munshi, S.K., Rahman, F., 2013. Influence of temperature on *Escherichia coli* growth in different culture media. J. Pure Appl. Microbiol. 7, 899–904.

Novak, M., 2015. Mathematical modelling as a tool for optimized PHA production. Chem. Biochem. Eng. Q. 29, 183–220. https://doi.org/10.15255/CABEQ.2014.2101.

Ochoa, S., Weiske, B., Simões, M.M., Neubauer, P., Riedel, S.L., 2025. Low-structured kinetic model of poly(3-hydroxybutyrate-co-3-hydroxyhexanoate) production from waste animal fats via fed-batch cultivations. Bioresour. Technol. 432. https://doi.org/10.1016/j.biortech.2025.132664.

Ochoa, S., Wozny, G., Repke, J.-U., 2010. A new algorithm for global optimization: Molecular-Inspired parallel tempering. Comput. Chem. Eng. 34, 2072–2084. https://doi.org/10.1016/j.compchemeng.2010.06.018.

Ochoa, S., Yoo, A., Repke, J., Wozny, G., Yang, D.R., 2007. Modeling and parameter identification of the simultaneous saccharification-fermentation process for ethanol production. Biotechnol. Prog. 23, 1454–1462. https://doi.org/10.1021/bp0702119.

Opheim, M., Šližyte, R., Sterten, H., Provan, F., Larssen, E., Kjos, N.P., 2015. Hydrolysis of Atlantic salmon (*Salmo salar*) rest raw materials - effect of raw material and processing on composition, nutritional value, and potential bioactive peptides in the hydrolysates. Process Biochem. 50, 1247–1257. https://doi.org/10.1016/j.procbio.2015.04.017.

Özilgen, M., 1988. Kinetics of amino acid production by over-producer mutant microorganisms. Enzym. Microb. Technol. 10, 110–114. https://doi.org/10.1016/0141-0229(88)90006-3.

Park, J.H., Lee, S.Y., 2010. Fermentative production of branched chain amino acids: a focus on metabolic engineering. Appl. Microbiol. Biotechnol. 85, 491–506. https://doi.org/10.1007/s00253-009-2307-y.

Poccia, M.E., Beccaria, A.J., Dondo, R.G., 2014. Modeling the microbial growth of two *Escherichia coli* strains in a multi-substrate environment. Braz. J. Chem. Eng. 31, 347–354. https://doi.org/10.1590/0104-6632.20140312s00002587.

Shio, I., Nakamori, S., Sano, K., To, A., 1971. Fermentative Production of L-threonine. US3580810.

Song, J., Zhuang, M., Fang, Y., Hu, X., Wang, X., 2024. Self-regulated efficient production of L-threonine via an artificial quorum sensing system in engineered *Escherichia coli*. Microbiol. Res. 284, 127720. https://doi.org/10.1016/j.micres.2024.127720.

Thompson, M.W., Maurizi, M.R., 1994. Activity and specificity of Escherichia coli ClpAP protease in cleaving model peptide substrates. J. Biol. Chem. 269 (27), 18201–18208. https://doi.org/10.1016/S0021-9258(17)32435-3.

Vélez Blandón, J.F., Sánchez Henao, C.P., Zapata Montoya, J.E., Ochoa, S., 2023. L-Threonine production from whey and fish hydrolysate by *E. coli ATCC® 21277™*. Heliyon 9, e18744. https://doi.org/10.1016/j.heliyon.2023.e18744.

Villamil, O., Váquiro, H., Solanilla, J.F., 2017. Fish viscera protein hydrolysates: production, potential applications and functional and bioactive properties. Food Chem. https://doi.org/10.1016/j.foodchem.2016.12.057.

Wanga, J., Cheng, L.K., Chen, N., 2014. High-level production of L-threonine by recombinant *Escherichia coli* with combined feeding strategies. Biotechnol. Biotechnol. Equip. 28, 495–501. https://doi.org/10.1080/13102818.2014.927682.

Xie, X., Liang, Y., Liu, H., Liu, Y., Xu, Q., Zhang, C., Chen, N., 2014. Modification of glycolysis and its effect on the production of l-threonine in *Escherichia coli*. J. Ind. Microbiol. Biotechnol. 41, 1007–1015. https://doi.org/10.1007/s10295-014-1436-1.

Yang, H., Hou, Y.-J., Xu, J.-Z., Zhang, ·wei-Guo, 2024. Metabolic engineering of Escherichia coli for the efficient production of L-threonine. Syst. Microbiol. Biomanuf. 4 (2), 810–819. https://doi.org/10.1007/s43393-023-00183-2.

Zafar, S., Owais, M., Saleemuddin, M., Husain, S., 2005. Batch kinetics and modelling of ethanolic fermentation of whey. Int. J. Food Sci. Technol. 40, 597–604. https://doi.org/10.1111/j.1365-2621.2005.00957.x.

Zapata Montoya, J.E., Franco Sanchez, A., 2022. The hydrolysates from fish by-product, an opportunity increasing. https://doi.org/10.5772/intechopen.102348.

Zhao, G., Zhang, D., Tang, Y., Hu, X., Wang, X., 2025. Recent advances on engineering *Escherichia coli* and *Corynebacterium glutamicum* for efficient production of L-threonine and its derivatives. Metab. Eng. 90, 1–15. https://doi.org/10.1016/j.ymben.2025.02.012.

Zhu, J., Shimizu, K., 2005. Effect of a single-gene knockout on the metabolic regulation in *Escherichia coli* for D-lactate production under microaerobic condition. Metab. Eng. 7, 104–115. https://doi.org/10.1016/j.ymben.2004.10.004.

Zoppellari, F., Bardi, L., 2013. Production of bioethanol from effluents of the dairy industry by *Kluyveromyces marxianus*. N. Biotech. 30, 607–613. https://doi.org/10.1016/j.nbt.2012.11.017.